Study of Different Roles Phosphorescent Material Played in Different Positions of Organic Light Emitting Diodes

Gu Keke, Zhong Jian*, Chen Jiule, Chen Yucheng, and Deng Ming

State Key Laboratory of Electronic Thin Films and Integrated Devices, School of Optoelectronic Information, University of Electronic Science and Technology of China (UESTC), Chengdu 610054, P. R. China

Phosphorescent materials are crucial to improve the luminescence and efficiency of organic light emitting diodes (OLED), because its internal quantum efficiency can reach 100%. So the studying of optical and electrical properties of phosphorescent materials is propitious for the further development of phosphorescent OLED. Phosphorescent materials were generally doped into different host materials as emitting components, not only played an important role in emitting light but also had a profound influence on carrier transport properties. We studied the optical and electrical properties of the blue 4,4′-bis(2,2-diphenylvinyl)-1,1′-biphenyl (DPVBi)-based devices, adding a common yellow phosphorescent material bis[2-(4-*tert*-butylphenyl)benzothiazolato-$N,C2'$] iridium(acetylacetonate) [(t-bt)$_2$Ir(acac)] in different positions. The results showed (t-bt)$_2$Ir(acac) has remarkable hole-trapping ability. Especially the ultrathin structure device, compared to the device without (t-bt)$_2$Ir(acac), had increased the luminance by about 60%, and the efficiency by about 97%. Then introduced thin 4,4′-bis(carbazol-9-yl)biphenyl (CBP) host layer between DPVBi and (t-bt)$_2$Ir(acac), and got devices with stable white color.   © 2013 The Japan Society of Applied Physics

1. Introduction

Since 1987, Tang[1] reported the first double layers organic light-emitting diode (OLED), OLEDs have been drawing more and more attentions because of their enormous potential for flat panel display and illumination. After decades of development, efficiency, lifetime and other properties of OLEDs have made tremendous progress. Especially the phosphorescent OLEDs, due to efficient use of the triplet excitons for electroluminescence,[2] could achieve extremely high luminance and efficiency for OLEDs commercialization. Commonly phosphorescent emitting materials were doped in suitable host materials, which could reduce the concentration quenching to receive high luminance and efficiency.[3–5] The host materials must have higher triplet energy than phosphorescent materials. In addition to use doping method, ultrathin emitting layers structure is also one way to decrease the quenching.[6,7]

But some studies showed phosphorescent materials not only can be used as emitting materials but also have other abilities. For instance, different doping concentration ratio of host-guest materials could affect the carrier injection and transportation property.[8,9] Chiu[10] inserted bis(3,5-difluoro-2-(2-pyridyl)phenyl-(2-carboxypyridyl)iridium(III) (FIrpic) into different positions of the device. Study concluded Firpic has four abilities as follows: 1 could help electrons inject from transporting layer to emitting layer; 2 could help transport electrons; 3 at low doping concentration ratio (3–6%), could help holes inject; 4 could act as hole trap, which can decelerate holes transport. Some phosphorescent materials exhibited carrier transporting properties as compared with traditional transporting materials.[11,12] Also some can be used to block and trap carriers.[13–15] Seunguk[14] demon-

strated 4,4′,4″-tris(carbazol-9-yl)triphenylamine (TCTA) doping with tris(2-phenylpyridine)iridium(III) [Ir(ppy)$_3$] could enhance electron transport ability, and reduce hole transport ability to 10^{-4}–10^{-6} cm^2 V^{-1} s^{-1} level. Baek[16] found the device with CBP doped 6% Ir(ppy)$_3$ has greatly improved carrier transporting abilities compared to CBP only device. Then based on each single color device carrier transporting properties, they fabricated white OLED with much better carrier balance.

The carrier balance is one of the most important factors for efficient OLED devices. The precise arrangement of each emitting component can balance carrier and stable color, which is the same as appropriate choosing of hole and electron transport materials, and eventually can effectively improve the performance of the device.[17] Bis[2-(4-*tert*-butylphenyl)benzothiazolato-$N,C2'$] iridium(acetylacetonate) [(t-bt)$_2$Ir(acac)] was known as efficient yellow phosphorescent material.[7] In this study, carrier transport properties and luminescence properties of (t-bt)$_2$Ir(acac) were investigated.

2. Experimental Procedure

Indium tin oxide (ITO) anode substrates with sheet resistance of 10 Ω/sq were pre-cleaned with detergent, deionized water, acetone, ethanol, for 15 min at each ultrasonic step, and then dried in a N$_2$ flow. Then the substrates were treated by oxygen plasma under a pressure of 25 Pa for 5 min to increase work function.[18] Organic functional layers were thermo-evaporated in vacuum with a pressure of 10^{-4} Pa, at deposition rate around 0.5–2 Å/s. After that, metallic cathode was deposited at rate of 3–5 Å/s without breaking the vacuum circumstances.

Devices used N,N'-bis(naphthalen-1-yl)-N,N'-bis(phenyl)-benzidine (NPB) as the hole transport material; 4,7-diphenyl-1,10-phenanthroline (Bphen) as the electron
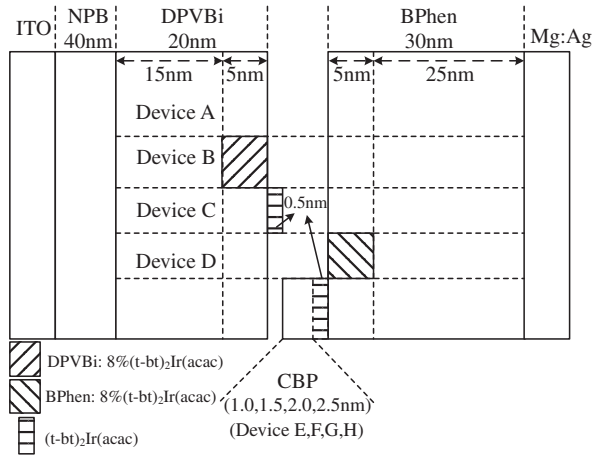
*E-mail address: zhongjian@uestc.edu.cn

Fig. 1.   Structures of devices.

Fig. 2.   Luminance–drive and current density–drive character curves of devices A–D.

transport material; 4,4′-bis(2,2-diphenylvinyl)-1,1′-biphenyl (DPVBi) as the blue emitting material; 4,4′-bis(carbazol-9-yl)biphenyl (CBP) as the host material. Cathode was 110 nm Mg:Ag (10 : 1) alloy. The structures are shown in Fig. 1. Devices were fabricated to be with structures as follows:

- A: ITO/NPB (40 nm)/DPVBi (20 nm)/Bphen (30 nm)/ Mg:Ag
- B: ITO/NPB (40 nm)/DPVBi (15 nm)/DPVBi:$(t$-bt$)_2$-Ir(acac) (5 nm, 8%)/Bphen (30 nm)/Mg:Ag
- C: ITO/NPB (40 nm)/DPVBi (20 nm)/$(t$-bt$)_2$Ir(acac) (0.5 nm)/Bphen (30 nm)/Mg:Ag
- D: ITO/NPB (40 nm)/DPVBi (20 nm)/BPhen:$(t$-bt$)_2$-Ir(acac) (5 nm, 8%)/Bphen (25 nm)/Mg:Ag
- E–H: ITO/NPB (40 nm)/DPVBi (20 nm)/CBP (x nm)/$(t$-bt$)_2$Ir(acac) (0.5 nm)/Bphen (30 nm)/Mg:Ag $x =$ 1.0, 1.5, 2.0, 2.5

Luminance–current density–bias voltage characteristics were tested simultaneously by combining the spectrometer with a Keithley 4200 semiconductor characterization system. Electroluminescence (EL) spectra and Commission International de l'Eclairage (CIE-1931) coordinates of the devices were measured by an OPT-2000 and PR650 spectrometer. All experiments were carried out at room temperature environment.

3.   Results and Discussion

Figure 2 shows the luminance–drive character curves of devices A–D. Devices B–D all showed better performance than none $(t$-bt$)_2$Ir(acac) device A. Especially device C with ultrathin $(t$-bt$)_2$Ir(acac) layer had the max luminance 6873 cd/m^2 at 11.8 V, and increased the luminance by about 60% compared to device A. As we can see from Fig. 3. Energy level diagrams, HOMO energy level of emitting material DPVBi and electron transport material BPhen is 5.9 eV[19] and 6.4 eV,[20] respectively, which both have a wide gap between $(t$-bt$)_2$Ir(acac) HOMO energy level 5.2 eV.

So after hole carriers transported to $(t$-bt$)_2$Ir(acac), it's difficult to transport out to EML and ETL because of the large barrier. Hence $(t$-bt$)_2$Ir(acac) can be regarded as a hole trap. Generally, hole mobility was much higher than electron
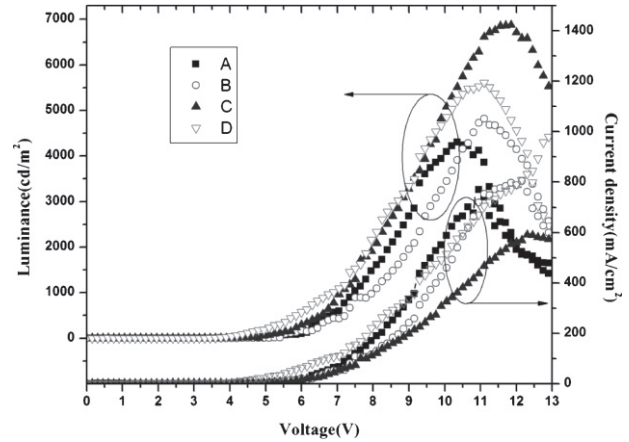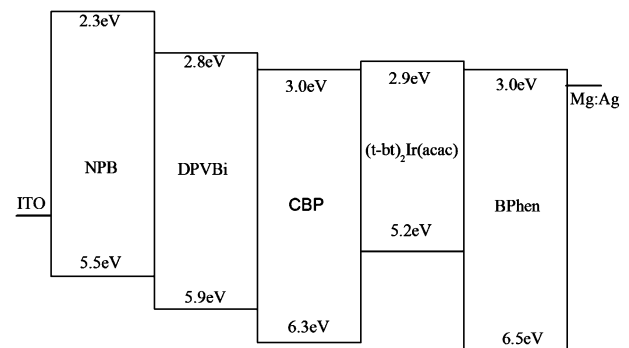

Fig. 3.   Energy level diagrams of the materials.

mobility in organic materials,[21] and that made holes majority carrier. So, devices B–D with $(t$-bt$)_2$Ir(acac) as hole trap, which could reduce holes and balance the carriers, had better performance. Conclusion $(t$-bt$)_2$Ir(acac) could act as hole trap can be proven by Fig. 2 the current density–drive character curves. Device C has the lowest current density and the largest luminance, demonstrated $(t$-bt$)_2$Ir(acac) could efficiently trap holes and balance carriers. The current densities of devices B and D were not as low as device C, that's because the doping ratio of devices B and D was high, $(t$-bt$)_2$Ir(acac) hole trap affection was weakened and acted more as emitting materials, which can be proven by Fig. 4 the spectra of devices.

Figure 4 shows the spectra of devices. Spectra of device A represents the spectra of DPVBi which can be seen has a 449 nm spectra peak, while spectra of device C had a 459 nm peak. Compared to device A, devices B–D all more or less had $(t$-bt$)_2$Ir(acac) emission spectrum. The 10 nm red-shift of the spectra was caused by the emission of $(t$-bt$)_2$Ir(acac). At low driven voltage, hole trap effect of $(t$-bt$)_2$Ir(acac) was dominant, thus the light of $(t$-bt$)_2$Ir(acac) could be neglected. As the voltage increased, $(t$-bt$)_2$Ir(acac) emission was just slightly enhanced. The reason why $(t$-bt$)_2$Ir(acac) emission couldn't be enhanced significant was the triplet energy of DPVBi is higher than $(t$-bt$)_2$Ir(acac), so the triplet excitons of $(t$-bt$)_2$Ir(acac) which could able to
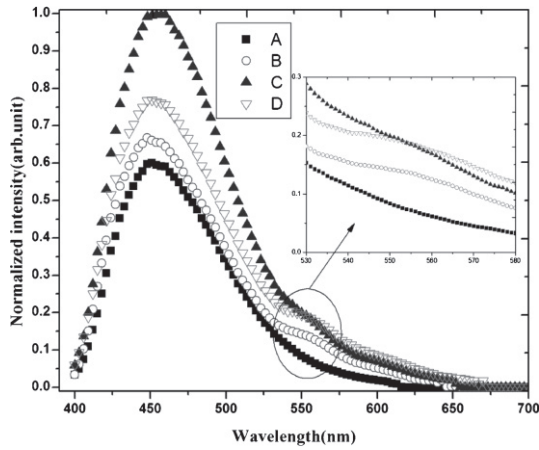
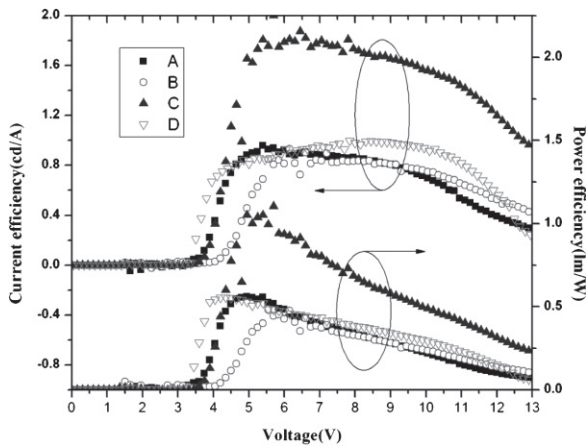Fig. 4.　Electroluminescence spectra of devices A–D at 10 V.

Fig. 5.　Current efficiency–drive and power efficiency–drive characteristics of devices A–D.

Fig. 6.　Current density–drive character curves of hole-only and electron-only devices.

employ triplets to emit phosphorescent yellow light, mostly transported to DPVBi which could not take advantage of triplets to emit light. Meanwhile, at high driven voltage $(t\text{-bt})_2\text{Ir(acac)}$ would snatch electrons from DPVBi and recombined with holes to form excitons, so devices B and D with high doping radio had not improved the performance, which can be seen from Fig. 5. Compared with the heavy doping devices, the thickness of ultrathin $(t\text{-bt})_2\text{Ir(acac)}$ layer was only 0.5 nm, which was not too thick to impede carrier transporting[22] and snatch lots of electrons.

Figure 5 shows current efficiency-voltage and power efficiency-voltage characteristics. Device C with an ultrathin layer had the best performance, and max current efficiency and power efficiency were 1.874 cd/A and 1.104 lm/W at 5.7 V, respectively. Device C had increased the current efficiency and the power efficiency by about 93 and 97% compared to device A, respectively.

To verify hole trap ability of $(t\text{-bt})_2\text{Ir(acac)}$, we fabricated hole-only devices and electron-only devices. Both hole-only devices and electron-only devices were divided into two devices, respectively, with or without $(t\text{-bt})_2\text{Ir(acac)}$. The structures were as follows:
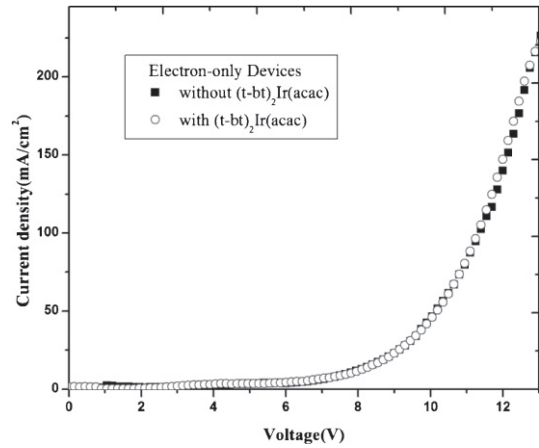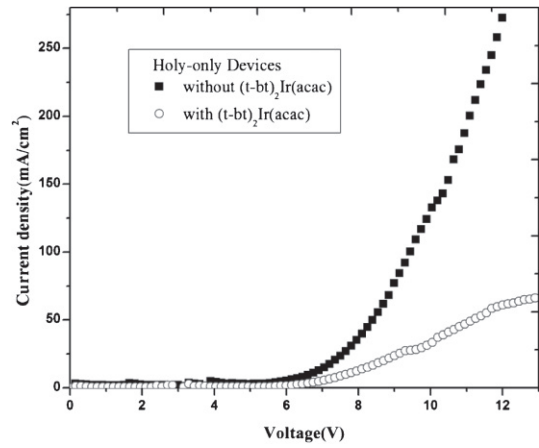
Hole-only devices: ITO/NPB (40 nm)/DPVBi (20 nm)/ with or without $(t\text{-bt})_2\text{Ir(acac)}$ (0.5 nm)/BPhen (30 nm)/ Ag (10 nm)/Mg:Ag

Electron-only devices: ITO/BPhen (10 nm)/NPB (40 nm)/ DPVBi (20 nm)/with or without $(t\text{-bt})_2\text{Ir(acac)}$ (0.5 nm)/ BPhen (30 nm)/Mg:Ag

Figure 6 shows current density–drive character curves of hole-only and electron-only devices. Hole-only device with $(t\text{-bt})_2\text{Ir(acac)}$ had lower current density than that without $(t\text{-bt})_2\text{Ir(acac)}$, meanwhile electron-only device with $(t\text{-bt})_2\text{Ir(acac)}$ had almost the same current density with the corresponding device at same voltage. The result proved $(t\text{-bt})_2\text{Ir(acac)}$ could trap holes, causing lower current density of hole-only device, and also indicated $(t\text{-bt})_2\text{Ir(acac)}$ had little effect on electron injection and transport.

$(t\text{-bt})_2\text{Ir(acac)}$ as a hole trap could enhance device luminance and efficiency. However, the recombination zone of the device was at the DPVBi/BPhen interface where $(t\text{-bt})_2\text{Ir(acac)}$ was located, so $(t\text{-bt})_2\text{Ir(acac)}$ also participated emitting light which would affect the color purity. Devices of ITO/NPB/$(t\text{-bt})_2\text{Ir(acac)}$/DPVBi/BPhen/Mg:Ag with optimized thickness of ultrathin $(t\text{-bt})_2\text{Ir(acac)}$ layer which is far away from the recombination zone, should have better performance without any yellow light. It is innovative to
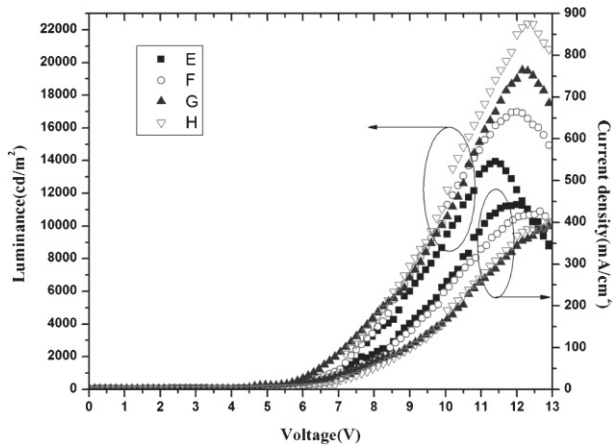
Fig. 7.   Luminance–drive and current density–drive character curves of devices E–H.
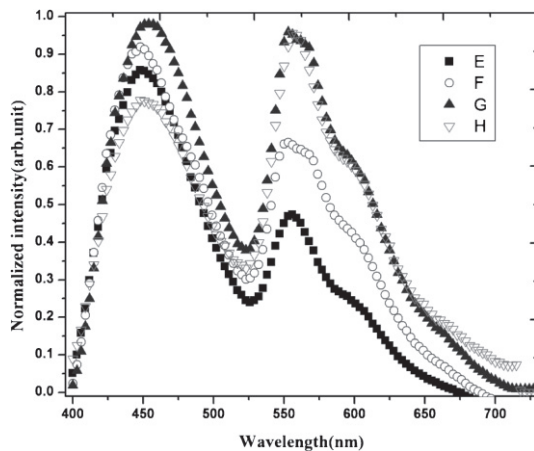

Fig. 9.   Current efficiency–drive and power efficiency–drive characteristics of devices E–H.

Fig. 8.   Electroluminescence spectra of devices E–H at 14 V.

Fig. 10.   Color coordinates of devices E–H.

use phosphorescent material $(t\text{-}bt)_2Ir(acac)$ to enhance the performance of fluorescent material DPVBi.

Afterward, we inserted different thicknesses CBP layers between DPVBi and $(t\text{-}bt)_2Ir(acac)$ to resist triplets transporting to DPVBi. Therefore $(t\text{-}bt)_2Ir(acac)$ known as efficient phosphorescent material could make use of the triplets to emit yellow light. Then by balancing blue fluorescence and yellow phosphorescence, devices could obtain white light emitting. Devices E, F, G, and H represent devices with 1.0, 1.5, 2.0, and 2.5 nm CBP layer, respectively.

Luminance–drive and current density–drive character curves are shown in Fig. 7. Clearly the luminance of the devices E–H increased with the increase of the CBP thickness. Figure 8 spectra of devices displayed two main emission peaks at 449 nm came from DPVBi and 556 nm with one shoulder peak at 595 nm came from $(t\text{-}bt)_2Ir(acac)$. Also we can see from the spectra of devices, thicker the CBP layer was, the greater proportion of yellow light was and the smaller proportion of blue light was. These indicated that emitting of $(t\text{-}bt)_2Ir(acac)$ was on the rise as the thickness of CBP increased. That was because the recombination zone

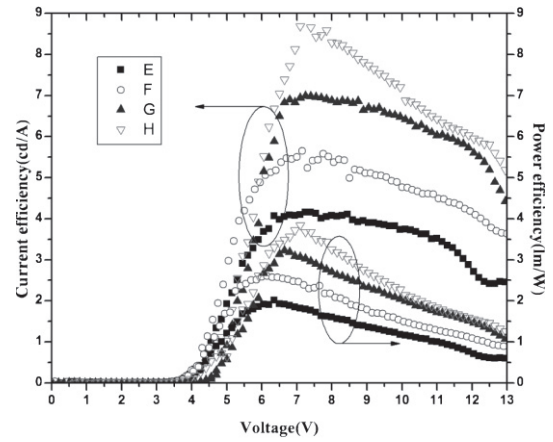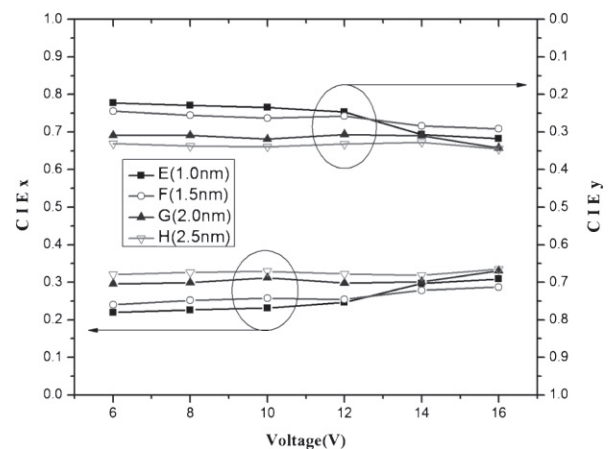which was located in CBP layer was gradually close to $(t\text{-}bt)_2Ir(acac)$ as the thickness of CBP increased. Then more triplet excitons could be transported to $(t\text{-}bt)_2Ir(acac)$ to emit. Since $(t\text{-}bt)_2Ir(acac)$ is one more efficient material than DPVBi, thicker the CBP layer was, better performance of the device should have.

Figure 9 current efficiency–drive and power efficiency–drive characteristics are consistent with the assumption. The max current efficiency and power efficiency of device H are 8.70 cd/A, 3.84 lm/W at 7.1 V, respectively. The efficiencies were not quite high. That is because on one hand undoped fluorescent DPVBi was not competent enough, on the other hand the thickness of each functional layer had not been optimized.

On account of the concentration quenching, roll off of the white devices was unsatisfactory. But color coordinates of devices G and H shown in Fig. 10 only had minor changes, especially device H. CIE values of device H changed from $(0.3205, 0.3308)$ at 6 V to $(0.3293, 0.3390)$ at 10 V to $(0.3348, 0.3452)$ at 16 V. Figure 11 CIE coordinates gives us an overall picture of the light color and the color changes. Judging from the figures, device E–H all have nearly white
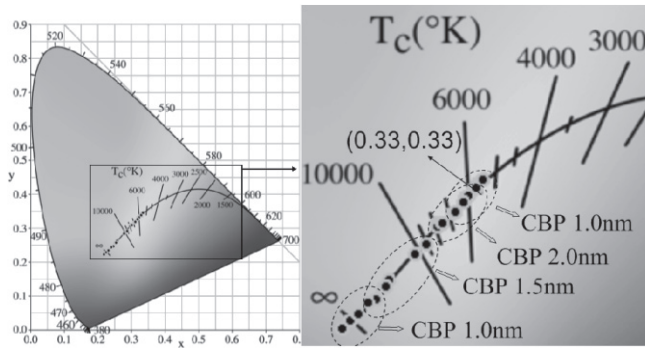
Fig. 11.　CIE coordinates of devices E–H.

light and good color stabilities. The changes of color also indicated the yellow light from $(t\text{-bt})_2\text{Ir(acac)}$ was gradually increased, which was consistent with the above analysis.

4.　Conclusions

In conclusion, based on the simple structure of blue fluorescent device of ITO/NPB/DPVBi/BPhen/Mg:Ag, we investigated carrier transport property of $(t\text{-bt})_2\text{Ir(acac)}$ through studying photoelectric properties of devices with $(t\text{-bt})_2\text{Ir(acac)}$ in different positions. The results indicated $(t\text{-bt})_2\text{Ir(acac)}$ could act as a hole trap, and inserting ultrathin layer in hole-wealthy structure could balance carriers, and improve the performance. Then introduced thin CBP layer between DPVBi and $(t\text{-bt})_2\text{Ir(acac)}$, and got color stable white devices. Although the efficiencies of these devices need to be elevated, we can conclude that we need to attach importance to the carrier properties of emitting materials, and the right arrangement of all emitting materials can greatly improve the performance of devices with two or more emitting layers.

References

1) C. W. Tang and S. A. VanSlyke: Appl. Phys. Lett. **51** (1987) 913.
2) Q. Wang, J. Yu, J. Zhao, J. Wang, M. Li, and Z. Lu: J. Lumin. **134** (2013) 870.
3) C. Weichsel, S. Reineke, M. Furno, B. Lüssem, and K. Leo: J. Appl. Phys. **111** (2012) 033102.
4) P. A. Levermore, A. B. Dyatkin, Z. Elshenawy, H. Pang, J. Silvernail, E. Krall, R. C. Kwong, R. Ma, M. S. Weaver, J. J. Brown, X. Qi, and S. R. Forrest: J. Photonics Energy **2** (2012) 021205.
5) K. S. Yook, S. O. Jeon, C. W. Joo, J. Y. Lee, M. S. Kim, H. S. Choi, S. J. Lee, C.-W. Han, and Y. H. Tak: Org. Electron. **10** (2009) 681.
6) J.-R. Koo, S. J. Lee, G. W. Hyung, D. W. Im, H. S. Yu, J.-H. Park, K. H. Lee, S. S. Yoon, W. Y. Kim, and Y. K. Kim: AIP Adv. **2** (2012) 012117.
7) X. Wang, J. Yu, J. Zhao, and X. Lei: Displays **33** (2012) 191.
8) Y.-H. Lan, C.-H. Hsiao, P.-Y. Lee, Y.-C. Bai, C.-C. Lee, C.-C. Yang, M.-K. Leung, M.-K. Wei, T.-L. Chiu, and J.-H. Lee: Org. Electron. **12** (2011) 756.
9) J. Zou, H. Wu, C.-S. Lam, C. Wang, J. Zhu, C. Zhong, S. Hu, C.-L. Ho, G.-J. Zhou, H. Wu, W. C. H. Choy, J. Peng, Y. Cao, and W.-Y. Wong: Adv. Mater. **23** (2011) 2976.
10) T.-L. Chiu and P.-Y. Lee: Int. J. Mol. Sci. **13** (2012) 7575.
11) W. H. Choi, C. H. Cheung, and S. K. So: Org. Electron. **11** (2010) 872.
12) C. Adachi, R. Kwong, and S. R. Forrest: Org. Electron. **2** (2001) 37.
13) N. Matsusue, S. Ikame, Y. Suzuki, and H. Naito: J. Appl. Phys. **97** (2005) 123512.
14) S. Noh, C. K. Suman, Y. Hong, and C. Lee: J. Appl. Phys. **105** (2009) 033709.
15) T.-L. Chiu, J.-H. Lee, Y.-P. Hsiao, C.-F. Lin, C.-C. Chao, M.-K. Leung, D.-H. Wan, H.-L. Chen, and H.-C. Ho: J. Phys. D **44** (2011) 095102.
16) H. I. Baek and C. H. Lee: J. Phys. D **41** (2008) 105101.
17) F. Lindla, M. Boesing, C. Zimmermann, P. van Gemmern, D. Bertram, D. Keiper, M. Heuken, H. Kalisch, and R. H. Jansen: J. Photonics Energy **1** (2011) 011013.
18) J. Huang, J. Yu, H. Lin, and Y. Jiang: J. Appl. Phys. **105** (2009) 073105.
19) H.-S. Jeon, H.-S. Oh, and S.-B. Yoon: Trans. Electr. Electron. Mater. **11** (2010) 145.
20) X. Lei, J. Yu, L. Zhang, Z. Ma, and Y. Jiang: Jpn. J. Appl. Phys. **50** (2011) 122102.
21) X. Xing, L. Zhang, R. Liu, S. Li, B. Qu, Z. Chen, W. Sun, L. Xiao, and Q. Gong: ACS Appl. Mater. Interfaces **4** (2012) 2877.
22) S. Liu, J. Yu, Z. Ma, and J. Zhao: J. Lumin. **134** (2013) 665.